Journal of Cleaner Production 425 (2023) 139051

Contents lists available at ScienceDirect

Journal of Cleaner Production

journal homepage: www.elsevier.com/locate/jclepro

Sustainable production of hydrogen, pyridine and biodiesel from waste-to-chemicals valorization plant: Energy, exergy and CO_2-cycle analysis

Andrea Liberale Rispoli, Chiara Tizzano, Nicola Verdone, Valentina Segneri *, Giorgio Vilardi

"Sapienza" University of Rome, Dept. of Chemical Engineering Materials Environment, via Eudossiana 18, 00184, Rome, Italy

ARTICLE INFO

Handling Editor: Mingzhou Jin

Keywords:
Waste-to-chemical
Process simulation
Environmental
Biodiesel
Pyridine.

ABSTRACT

This study deals with the simulation of waste-to-chemicals plant for the conversion of municipal solid waste to hydrogen, biodiesel and pyridine. The study analyses a Waste to Chemical plant, in order to evaluate the future scenarios of the integrated management of municipal waste from a technical and economic point of view and compare them, both in terms of material flows and related costs. In a first phase, the characteristics of the simulation model created with the help of the Aspen Plus software are analysed. Subsequently, with the help of a calculation model, the operating costs, emissions and energy and exergy efficiency are evaluated for the two identified scenarios.

Starting from about 3000 t/h of waste, as a main result, about 8.4 t/h of pyridine and 300 t/h of biodiesel are produced and about 7.94 t/h of H_2 as a by-product. The main purpose of the design cycle is to reduce the amount of waste to landfill, valorising it and limiting CO_2 emitted in the atmosphere at the same time.

Two system configurations are considered to maximize the reuse of all waste streams. In particular, the comparison was made between two scenarios: in the first the stream separated by extraction is considered a waste for the plant, while in the second scenario, this stream is sent to a fermentation section to obtain an excess bioethanol stream, which represents another product with high added value. The treatment of the stream separated from the extraction in the second scenario allows to obtain an additional stream of bioethanol in addition to the target products.

A complete energy, exergy, environmental and economic analysis of the simulated plant have been carried out. The work shown that in the second case the waste exergy is dramatically reduced, leading to a raise of exergy efficiency from 30.2% up to 84.9%. While, from the environmental point of view both scenarios have low CO_2 emissions, 0.52 $kgCO_2/kg$ products and 0.87 $kgCO_2/kg$ products respectively.

1. Introduction

Nowadays, the problem of the waste disposal and the possible conversion of the municipal solid waste (MSW) to energy or chemical products is a crucial point in the theme of energy transition. Still today, one of the most common way to manage waste is landfilling, that usually is the worst method to work off MSW both from the economical and the environmental point of view; indeed, for example, in Italy almost 44% of the MSW is sent to landfill and in US landfilling is still reported as one of the major way with which the MSW are managed (Brunner and Rechberger, 2015; El-Fadel et al., 1997; Psomopoulos et al., 2009).

There are two routes for the waste management that must be covered in the early future and that have already been explored; the first one is the MSW conversion to energy through incineration or other processes (Beiron et al., 2020; Tang et al., 2020). This process is the well-known "waste to energy" way and a notable number of industrial plants are present in all developed countries (Brunner and Rechberger, 2015).

This kind of process, which is at this point considered very proven, can be merged with a second one, in order to develop a plant that converts the whole CO_2 generated from the combustion of the MSW into a product that can be sold into the market. This rout will be more and more covered in the early future since the possibility of the removal of the exemption that waste to energy plants have for the carbon tax (European Council, 2010).

* Corresponding author.
E-mail address: valentina.segneri@uniroma1.it (V. Segneri).

https://doi.org/10.1016/j.jclepro.2023.139051
Received 23 November 2022; Received in revised form 24 September 2023; Accepted 26 September 2023
Available online 27 September 2023

One example of this merging to develop this kind of plant is reported in (Rispoli et al., 2021c): in this study the authors simulated a waste to energy plant implemented with a power to gas unit, to produce power from the combustion of the MSW and methane from the CO_2 generated from the combustion itself. This article also reports the energy and exergy efficiency, proving that is higher with respect to that of a waste to energy plant lacking the power to gas unit.

Another study made on the waste to energy plant was carried out by Islam (2016), analysing the impact of a waste to energy generation plant in two of the largest cities of Bangladesh, Dhaka and Chittagong. In this work the author reported how, in a context of lacking land resources, the waste to energy plant can improve the reducing of the carbon footprint of the country.

The second route for the management of the MSW consists of a thermo-chemical treatment of the waste with which it can be transformed into a chemical, most of the times into syngas, to have a starting point for most of the process in the modern chemical industry. The advantage of this kind of process is the possibility to use a syngas, which can be seen as a building block of the modern chemistry, that origins from a waste (that represents a secondary resource) and not from fossil primary sources. In this way, the carbon footprint of the process is reduced.

A solution for this kind of plant is reported in the work of Rispoli et al. (2021a) in which the MSW is fed into a gasifier to produce syngas; here this gas is then separated into pure hydrogen and a reducing gas used to substitute coal fines in a steel furnace. A decarbonization of both refinery plant and iron and steel plant was conducted, just as it was mentioned before.

Another possible solution belongs to this category of processes is the pyrolysis of the waste. This was analysed in the work made by Buah et al. (2007) and it was reported pyrolysis as an attractive alternative to incineration for MSW disposal. The pyrolysis process was performed in a fixed bed reactor, to recover the three phase products of the reaction: a solid char, a liquid oil/wax and combustible gases that have a suitable high heating value to be used as fuel. The temperature has a main role in this kind of process and the authors find as best working range 400–700 °C.

Another type of process that belongs to this category is that reported in the study by Zhao et al. (2022), which analyses the pyrolysis and gasification of waste (in particular of plastic waste) with the aim of producing high-value products: liquid fuel, H_2, nanomaterial, monomer, respecting the concept of Circular Economy.

According to the authors, in the early future the Waste to Chemical solution (this is called the way with which the waste is converted into a chemical product) will be very useful for the chemical industry: indeed, it is able to convert the MSW, that is in most of the case a cost for the country that have to work off it, into a new high added value product. Moreover, one of the most important advantages of this strategy is its carbon footprint, that is close to zero, since almost the totality of carbon contained in the MSW goes into the chemical (Rispoli et al., 2021a), like for example biodiesel and high-value chemicals such as azo-compounds.

Studying the potential of waste and biomass for generating sustainable bioenergy carves a pathway into a circular bioeconomy regime, and can help tackle our heavy reliance on non-renewable energy sources. The traditional linear economy model revolves around a disposal system, where products are not recycled at the end of their ‘useable’ life cycle. A circular bioeconomy, on the other hand, aims to achieve industrial symbiosis through the reuse of wastes or by-products from an industrial system. Using waste products, which would have traditionally been disposed of in landfills, to generate biofuels and high added value product for commercial and industrial use extends the materials’ life cycle (Escalante et al., 2022).

The present work deals with a strategy of municipal solid waste and organic waste disposal belonging to the second route (waste-to-chemicals). More in detail, the MSW is fed into a gasification reactor to produce syngas that is upgraded to hydrogen and fed with nitrogen into an ammonia reactor to produce ammonia. The nitrogen is from the Air Separation Unit (ASU) necessary to obtain the oxygen stream fed to the gasifier. The organic fraction of the MSW is fed in lipids extraction unit and then in a fermentation unit to produce ethanol; both ethanol and lipids are used to produce biodiesel and glycerol as by-product. Glycerol reacts in a dehydration unit to produce acrolein that reacts with ammonia to produce pyridine as final product.

Pyridine is a basic heterocyclic organic compound identified by the chemical formula C_5H_5N that has several applications in various field. One of the most important example of the uses of this molecule is the medical field: it can be used as anti-microbial, anti-viral, antioxidant, anti-diabetic and it has also some anti-cancer activities (Ali Altaf et al., 2015).

Biodiesel is an alternative of the diesel fuel, made by renewable biological sources, like vegetable oils. It became more attractive in last years since its environmental benefits (Ma and Hanna, 1997; S. Wang et al., 2020). Today, since biodiesel is mainly produced from vegetable oils, it is contained in the family of “first generation biofuel” and for this reason it goes to meet the controversies of the antagonism between the fuel area and the food area, since the land used to grow the palm to produce diesel can’t be used for the farming and so for feed the population (Martin, 2010). This debate food versus biofuel, which is quite delicate in world where many populations suffer hunger, can be overcome producing the fuel from the waste, as it will show later in this work, making biofuel belonging to the category of “advanced biofuel” (Cheng and Timilsina, 2011; X. Xu et al., 2015).

The proposed process can convert the whole feed of MSW and organic into a biofuel and a bio-chemical reducing in this way the carbon footprint. The whole process has been simulated in Aspen Plus environment and a complete energy, exergy, environmental and economic analysis has been carried out.

Techno-economic analysis attempts to link technological parameters of bioenergy and bioproduct systems with economic indicators and environmental impacts (Thomassen et al., 2019). This promising framework can be used for cost-benefit comparison and real-world implementation of bioenergy and bioproduct systems (Aghbashlo et al., 2022).

There are multiple articles reporting studies on different Waste to chemical processes, but currently there are no studies similar to the one presented here either in the scientific literature or on the basis of the industrial knowledge of the authors. The work presented is interesting and innovative thanks to the integration of two processes: gasification for the non-recyclable fraction of the waste, and an extraction and fermentation process for the organic fraction, to obtain the complete conversion of the waste into products with high added value, through an integrated, efficient and low-emissions process. Generally, many of the previous studies deal with analysing only a part of the waste, such as plastic waste, or organic waste. In this study, thanks to the combination of gasification and fermentation it is possible to obtain two products with high added value such as biodiesel and pyridine, as well as hydrogen and bioethanol as interesting by-products, managing to treat all the incoming waste, without having waste, with an integrated, flexible and efficient process.

2. Processes description

The proposed process is able to convert the entire feed (divided as 127 t/h of Refuse derived fuel, RDF, and 2800 t/h organic fraction of municipal solid waste, OFMSW, in the proposed scheme) in target products, biodiesel and pyridine, thanks to an integrated cycle. The size of the plant was set up considering the hourly production of OFMSW and RDF in Italy, of about 3000 t/h. RDF is fed into a gasification reactor to produce syngas and after purification and a step of water gas shift, is converted in hydrogen. This stream with a nitrogen one from an Air Separation Unit (ASU), is fed into ammonia synthesis section. Meanwhile, the ASU provides pure streams of nitrogen and oxygen. On the

other hand, the organic fraction of waste goes through step of lipids extraction and fermentation to produce bioethanol. Both, lipids and bioethanol, are used to produce biodiesel and glycerol as by-product. In the end, glycerol is dehydrated to acrolein that reacts with ammonia to produce pyridine in the final step. The process was divided into two scenarios. In fact, the traditional process (the first scenario) produced a post-extraction flow rate too high to obtain only the bioethanol useful for biodiesel synthesis, thus having a high waste flow rate that could be used again, because it still contained useful bioactive compounds. The target biodiesel productivity was 300 t/h, leading to a pyridine productivity of 8.4 t/h. For this reason, a second scenario was analysed, in which all the post-extraction current is used to produce an additional bioethanol stream, considered as a further product of the plant. A block diagram of the process is reported in Fig. 1, in which the waste stream which in the second scenario is converted into bioethanol is highlighted in red.

In the subsequent paragraphs each unit is described more in detail.

2.1. Process layout

The whole plant described in this paragraph is reported in the block diagram in Fig. 1 and it has been simulated in Aspen Plus® environment.

Two different thermodynamic systems have been adopted. For the compressors and for the vapour phase reactions, Peng – Robinson model was adopted; whereas NRTL – RK (Not Random Two Liquids, with cubic equation of Redlich – Kwong) was used for remaining operations.

2.1.1. Gasification and water gas shift

The waste is fed into a gasification reactor at a standard condition where it is converted in syngas and granulate that can represent a by-product. The feed of the plant (Refused Derived Fuel or RDF) (Agovino et al., 2016; Rispoli et al., 2021a) has a flowrate of 127 t/h and it is modelled as a non-conventional component, based on the analyses in the Table 1 (Grillo, 2013):

The gasifier reactor has been modelled based on previous work (Borgogna et al., 2019). In particular, the reactor is divided in 3 zones: melting zone in the bottom, gasification zone in the middle and stabilization zone on the top, as shown in Fig. 1A in supplementary material. A stream of oxygen is used as comburent while a stream of methane is used to provide the heat for reactions.

The subsequent section of the plant is the cleaning and the purification of the gas, where it is cooled down to 90 °C, to avoid the formation of toxic compound like furans (Safavi et al., 2021). Then, the separation of some dangerous compound like HCl, COS, HCN, H_2S occurs. The simulation of this part of the plant was carried out in a previous

Table 1
Ultimate analysis and Proximate analysis of waste entering in the reactor.

Ultimate Analysis of Waste		
	Value	Units
Ash	21	%
Carbon	30	%
Hydrogen	4	%
Nitrogen	0.5	%
Chlorine	0.5	%
Sulphur	0.3	%
Oxygen	20	%
Proximate Analysis of Waste		
	Value	Units
Moisture	23.7	%
Fixed Content	4	%
Volatile Matter	68.5	%
Ash	27.5	%

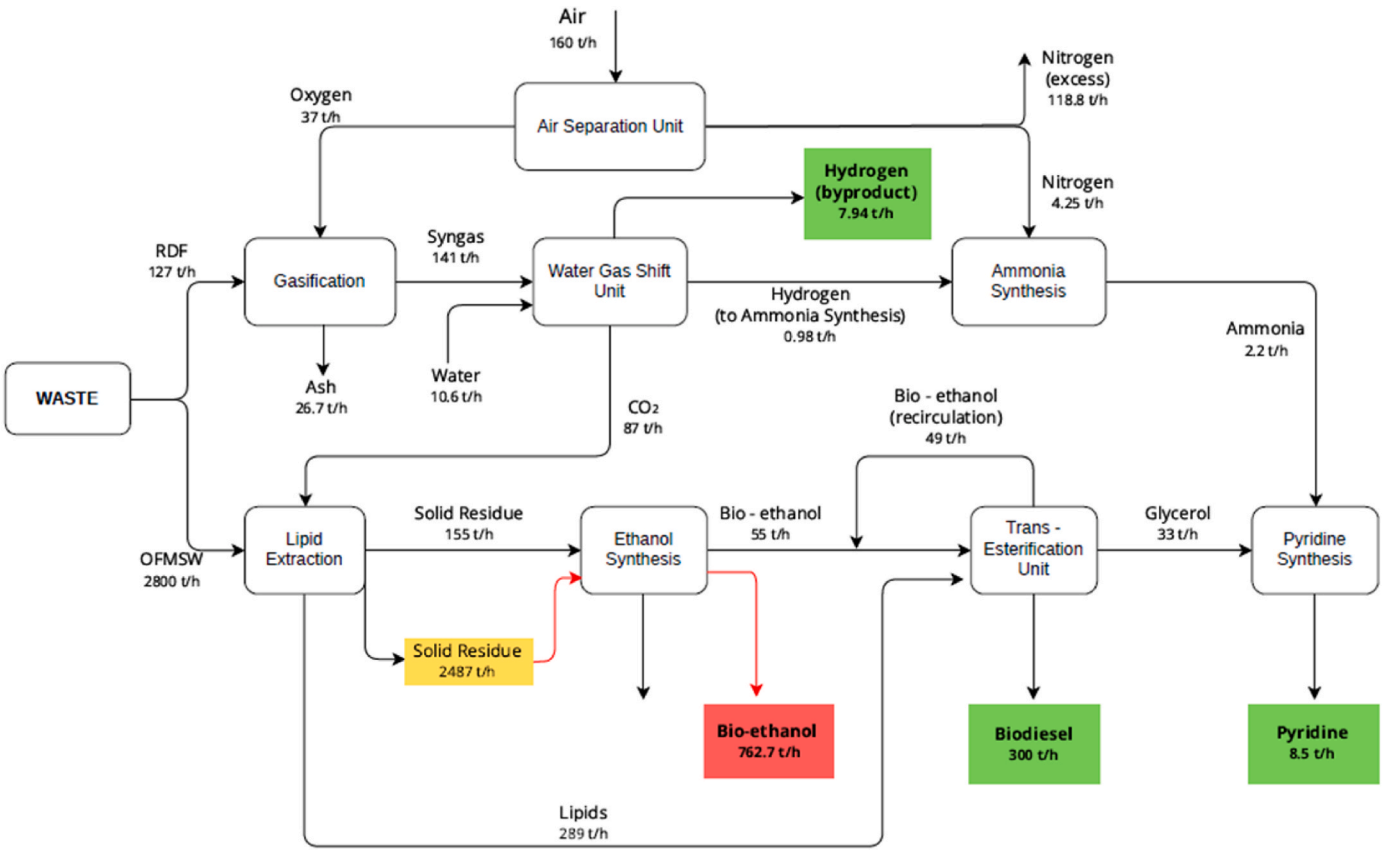

Fig. 1. Block diagram of the process.

work (Rispoli et al., 2021a).

The next step of the plant is the Water Gas Shift (WGS in Fig. 2) reaction (eq. (1)), where the hydrogen concentration in the gas is raised, by the conversion of the CO in CO_2 with the presence of water.

$$CO + H_2O \leftrightarrow CO_2 + H_2 \quad (1)$$

This reaction is simulated in an adiabatic Gibbs reactor and a pression of 1 atm, reported in Fig. 2.

The heat exchanger located before the mixer (E−2 in Fig. 2) is necessary to increase the temperature of the gas till 320 °C, optimal for the reaction (Borgogna et al., 2019), and it was realized with the syngas upstream the quench. The most important variable for the reaction is the H_2/CO ratio, which is maintained fixed equal to 3 manipulating the inlet water stream. Then, the gas is fed to a PSA unit (SEP-6 in Fig. 2) that operates at 15 atm (Rispoli et al., 2021a) where hydrogen with 99% of purity is separated by the remaining gas, composed mainly by CO_2. The hydrogen flowrate is sent to the ammonia synthesis section, whereas the CO_2 stream is fed to the lipids extractor. A certain amount of hydrogen is recovered as a by-product of the process.

The heat exchanger (E−4 in Fig. 2) is used to cool the CO_2 stream down to 130 °C, the inlet temperature to the compressor of the extraction section. This temperature was found through a preliminary optimization analysis regarding the maximum allowable temperature inside the multistage compressor adopted.

2.1.2. Ammonia synthesis

The hydrogen from the WGS section must be compressed up to 200 atm and heated up to 400 °C to allow the reaction with nitrogen and to form ammonia in the ammonia reactor (Cheema and Krewer, 2018). To do this, a multistage compressor is required, reported in Fig. 3A in supplementary material.

The device was projected using the following equation (2) (Lüdtke, 2004):

$$Rc_i = \sqrt[z_i+1]{Rc} \quad (2)$$

This is a simplified relationship that considers the interstage temperature equal to the inlet temperature of each.

In Fig. 3 the ammonia synthesis section of the plant is reported.

Ammonia is produced inside the Gibbs reactor (AMMONIA in Fig. 3), and it is separated through condensation in a flash after being cooled to 50 °C, while the pressure remains the same as in the reactor i.e., 200 atm. The gas portion of the stream is the recycle of the reactor (Cheema and Krewer, 2018).

2.1.3. Air separation unit

The air separation unit (represented in Fig. 2A in supplementary material) provides pure oxygen and nitrogen streams, useful in gasification and ammonia synthesis section. The separation is realized through a cryogenic distillation.

The inlet flowrate of air, which for simplicity has been taken as 21% mol oxygen and 79%mol nitrogen, is 5530 kmol/h. The feed is compressed to 4 atm, cooled to 47 °C trough the heat exchanger (E−1 in Fig. 2A) and divided in two fractions. The second one, is compressed again to 6 atm, i.e., the operating pressure of the column HPC (High Pressure Column). After the compression (C-2 in Fig. 2A) the temperature is reduced to 50 °C through a heat exchanger (E−2 in Fig. 2A). While the heat exchanger E−3 allows the liquefaction of air through heat recovery with the cold currents coming from the next distillation unit (Khalel et al., 2013).

After heat recovery (E−3 in Fig. 2A), there are two columns operating at different pressures but thermally coupled by a single heat exchange unit which acts as a reboiler of the low-pressure column and condenser of the high-pressure column. Both columns are simulated with a RadFrac blocks. The high-pressure column (HPC in Fig. 2A) has 15 stages and a reflux ratio of 0.53: it provides streams of pure nitrogen and oxygen enriched air that, after heat recovery, are used as a reflux of the low-pressure column (LPC in Fig. 2A). While, the LPC column has 20 stages and reflux ratio of 0.61 and provides pure nitrogen from the top and pure oxygen from the bottom. After, these currents reach the initial heat recovery unit (E−3 in Fig. 2A).

2.1.4. Organic fraction of municipal solid waste treatment section

In this section the organic fraction of municipal solid waste is treated. The Table 2 shown its composition (Barampouti et al., 2019):

Cellulose is entered as $C_6H_{10}O_5$, hemicellulose as $C_5H_8O_4$ whereas the lipids have been entered as an equimolar mixture of triglycerides (triolein, tripalmitin and trimyristin) (Ardila et al., 2014). The starch and the proteins have been included as solid component, specifying molecular weight and heat of formation according to the reaction in which they are involved. These properties are necessary for Aspen to perform material and energy balances.

The first step is the lipids extraction, this is realized with carbon dioxide obtained from the water gas shift section. Fig. 4A in supplementary material shows the multistage compressor useful to reach a pressure of 47 atm and heat exchanger (E−3 in Fig. 4A) that down up the temperature to 10 °C (Olguín et al., 2022).

After a first step of liquefaction, the carbon dioxide reaches its critical temperature and pressure conditions (31 °C, 73.8 atm) thanks to a pump (P-1 in Fig. 4A) and a heat exchanger (E−4 in Fig. 4A).

Fig. 4 shows the lipids extraction section.

The CO_2 stream is mixed with the organic fraction of MSW and fed to the lipid's extractor, modelled as a Gibbs reactor in Fig. 4. In this block, the yield of the component extracted is obtained. Based on literature data (C.S. Lim et al., 2003), an efficiency of 55% with a molar ratio of CO_2/lipids of 20 was entered as specific. This section represents the bottleneck of the process. In fact, due to these high molar ratios, a CO_2

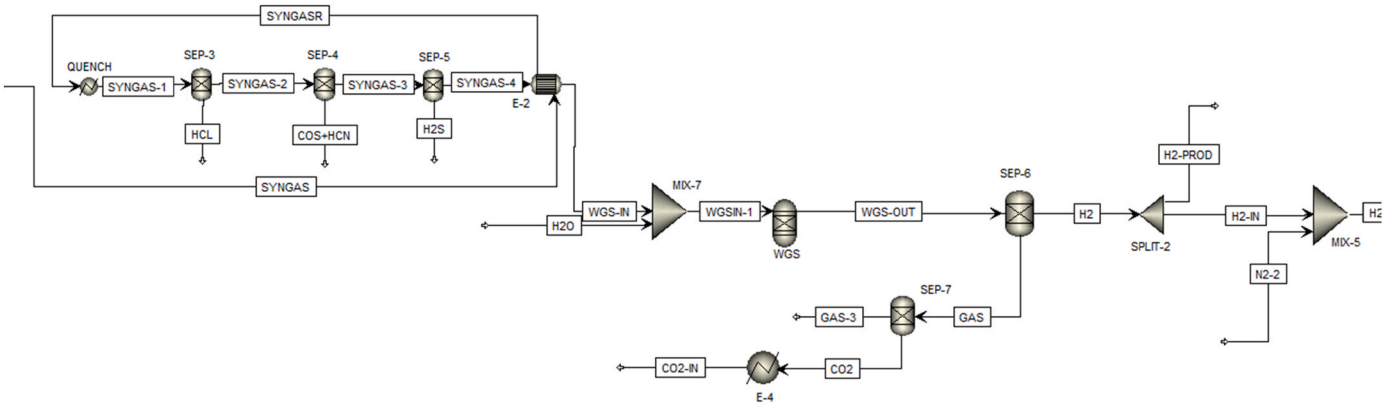

Fig. 2. Syngas cleaning and WGS section modelled on simulation software.

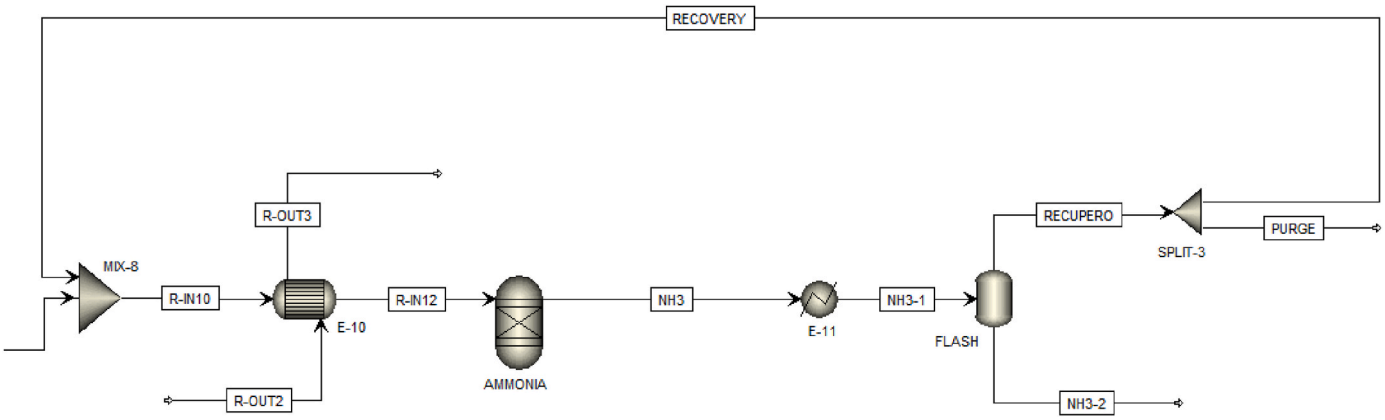

Fig. 3. Ammonia synthesis section modelled in the simulation software.

Table 2
Chemical Composition of organic fraction on dry bases.

Composition of the organic fraction		
	Value	Units
Lipids	19	%
Protein	16	%
Cellulose	21.55	%
Hemicellulose	15.65	%
Starch	27.8	%

flowrate of 10.54 kt/h, with a make-up of 87 t/h is necessary with respect to an organic feed of 2800 t/h. Once the compounds of interest have been obtained, the carbon dioxide stream must be separated and recirculated to the inlet of the extractor. The CO_2 stream is expanded to 47 atm and heated to 27 °C, obtaining a separation efficiency of 99.99%.

After lipids recovery, the solid residue is directed to the fermentation steps and two scenarios are identified. The target biodiesel flowrate is 300 t/h, and a net bioethanol flowrate of 55 t/h is required to produce it. This flowrate was obtained considering the alcohol/lipids ratio useful for the next transesterification section and the percentage of alcohol that can be recovered by distillation (94% by mass) after the above section. According to this, the first scenario deals with the production of 104 t/h of bioethanol (49 t/h of this are recirculated), leading to a considerable post extraction waste stream (2486 t/h) that could be further upgraded or valorised. Therefore, the second scenario deals with the production of additional 762.7 t/h of bioethanol, obtained from the conversion of the 2486 t/h of the waste stream.

Fig. 5A in supplementary material shows the bioethanol unit. The formation of bioethanol proceeds through 2 steps: hydrolysis and fermentation and the Tables 1A and 2A in supplementary material shown the reaction involved.

Hydrolysis reactions lead to the release of fermentable sugars and are carried out at 50 °C, temperature compatible with the micro-organisms present at this stage and at atmospheric pressure. In addition, a water stream also enters the reactor (SACCHAR in Fig. 5A), with a solids/water weight ratio of 0.2. A heat exchanger (E−7 in Fig. 5A) follows the reactor, to decrease the temperature to 32 °C, because of the micro-organisms used in the following reactor and, in this step, sugars are converted into alcohol and carbon dioxide. However, a secondary reaction also takes place, leading to the formation of higher alcohols.

As higher alcohols have been considered isoamyl alcohol, amyl alcohol and iso-butanol (Ferreira et al., 2013). These by-products (also called 'fusel oil') are separated by subsequent distillation as a side cut, considering their low concentration (<0.025%vol of bioethanol). At the exit of the fermentation section the digestate is separate i.e., all unreacted compounds that could still be used. The distillation (D-1 in Fig. 5A) with 30 stages and 5.98 as reflux ratio, is the last unit which allows to recover on the top the azeotrope water-ethanol. To reach the full grade specific (98% of purity), the ethanol must be dehydrated in a silica gel fixed bed separator (MOLSIEVE in Fig. 5A) (Onuki et al., 2016). Subsequently the water stream is recovered, cooled to 50 °C and combined with the incoming water stream in the hydrolysis section. Ethanol stream, on the other hand, is used to heat the water stream entering in the previously mentioned section, reaching a temperature of 60 °C, useful for the next transesterification step.

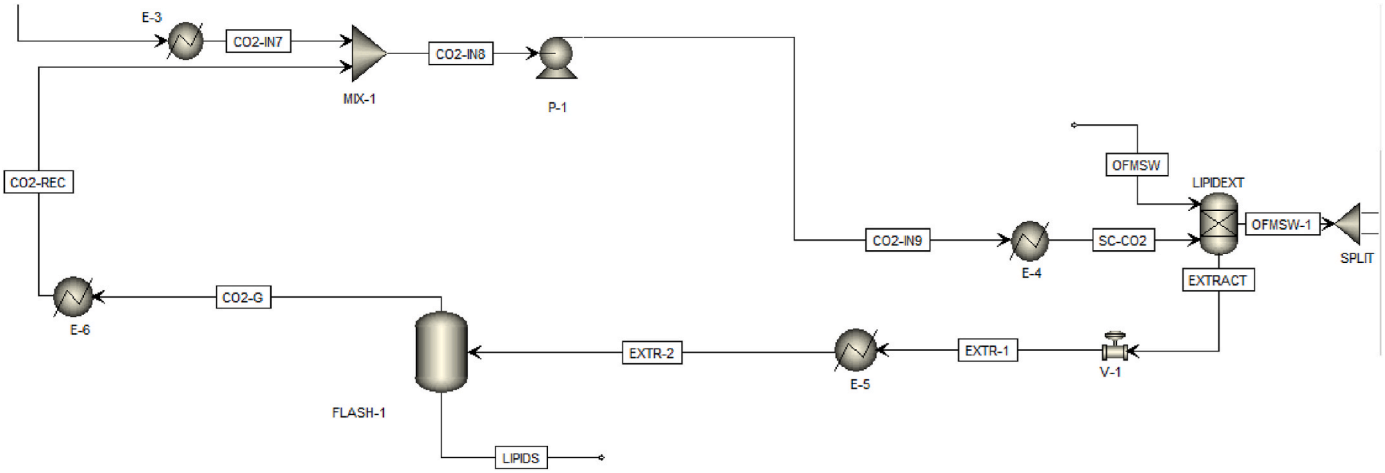

Fig. 4. Lipids extraction section modelled in the simulation software.

2.1.5. Biodiesel unit

Lipids and bioethanol produced by the extraction and fermentation section are fed to the biodiesel unit, represented in Fig. 5.

The lipids stream flowrate is 360 kmol/h, whereas the ethanol one is 2160 kmol/h, with a make-up of 1144 kmol/h. The ethanol flowrate has been calculated assuming a molar alcohol/oil ratio of 6 (Silva and de Andrade, 2020). The process uses an alkaline catalyst (KOH), guaranteeing a higher conversion with a shorter residence time. The percentage of catalyst in input is 1% by mass compared to the lipid stream.

Initially the fresh alcohol stream (1 atm, 60 °C) and the catalyst are mixed (MIX-1 in Fig. 5) and then pumped to the reactor that has an operating pressure of 1.4 atm. The lipid stream is mixed (MIX-3 in Fig. 5) with the recirculating stream from the biodiesel purification column. The reactor used is a CSTR and for this reason no preheating of the charge is necessary. Inside the reactor, transesterification reactions take place, and these have been modelled using second-order kinetics, as shown in equation (3) (Silva and de Andrade, 2020):

$$r = k_0 \exp\left(-\frac{E_a}{RT}\right) * C_a * C_b = k * C_a * C_b \quad (3)$$

The Table 3A in supplementary material shown the reaction involved and the kinetic parameter used (Silva and de Andrade, 2020).

The reactor has been simulated according to a residence time of 1.5 h, i.e., the optimal value basing on literature data (Silva and de Andrade, 2020), where it has been stated that the side saponification reaction can be neglected for residence time values $\leq$ 1.5 h.

The experimental data reported in the work of Agarwal et al. was used to validate the kinetic model (Agarwal et al., 2012).

A first distillation column (D-1 in Fig. 5) follows the reactor unit: it is characterized by 7 stages, a reflux ratio 1.98 and top pressure of 0.2 atm, to prevent the degradation of biodiesel and glycerol. Ethanol is then recovered from this unit and recirculated to the reactor. The pump (P-4 in Fig. 5) and the heat exchanger (E−1 in Fig. 5) bring the operating conditions to 60 °C and 1.1 atm. A liquid-liquid extraction is required to separate the by-product, i.e., the glycerol. The absorber column (WASH in Fig. 5) has been simulated with RadFrac block, with 6 stages and temperature on the top of 25 °C. The second distillation column (D-2 in Fig. 5), operating with 6 stages, 1.08 as reflux ratio and a pressure of 0.2 atm, enables the recovery of biodiesel. While the second liquid stream from the previous extraction goes to a neutralization step with phosphoric acid in a reactor operating at 50 °C and 1.1 atm. The reaction that takes place is reported in equation (4):

$$3\,KOH + H_3PO_4 \rightarrow K_3PO_4 + 3\,H_2O \quad (4)$$

The conversion of the hydroxide was considered complete.

Then a separator (FILTER in Fig. 5) recovers the aqueous glycerol phase to be sent to the following distillation section (D-3 in Fig. 5), operating with 6 stages, a reflux ratio of 1.99 and at 0.5 atm.

2.1.6. Pyridine synthesis

The pyridine synthesis section consists of a glycerol dehydration step, the acrolein purification and the production and purification section. In general, glycerol is used as an intermediate to produce pyridine.

Fig. 6A in supplementary material shows the glycerol dehydration section.

The glycerol stream leaving the biodiesel section at 262 °C and 0.5 atm, undergoes to a pre-cooling (E−1 in Fig. 6A) to 255 °C so that a pump (P-1 in Fig. 6A) can be used to increase the pressure to 1 atm, avoiding the need of a compressor. Heat recovery (E−2 in Fig. 6A) is then carried out, to reach the useful temperature of the reactor inlet which is a catalytic and adiabatic Plug Flow Reactor (PFR). The following reaction kinetics were implemented to model the glycerol dehydration step (Banu et al., 2015).

The reactions are (equations (6)–(9)):

$$C_3H_8O_3 \rightarrow C_3H_4O + 2H_2O \quad (6)$$

$$C_3H_4O \rightarrow CO + C_2H_4 \quad (7)$$

$$C_3H_4O \rightarrow 3C + H_2O + H_2 \quad (8)$$

$$C_3H_8O_3 \rightarrow C_2H_4O + H_2 + H_2O + CO \quad (9)$$

Table 4A in supplementary material shows the kinetic parameter of glycerol dehydration.

The kinetic parameters have been entered using an LHHW (Langmuir–Hinshelwood–Hougen–Watson) model, as shown in eq. (5):

$$r = k_0 \exp\left(\frac{-E_a}{RT}\right) * p_i \quad (5)$$

The kinetics are given for a specific type of catalyst, zeolite HZSM-5. The density of the catalyst and the degree of vacuum in the bed are also included: 720 kg/m^3 and 0.75 respectively (Banu et al., 2015).

The information of catalyst data is reported in Table 3.

The kinetic model was validated by replicating the experimental data reported in the work of Wang et al. (X. Wang et al., 2020). Sensitivity analyses are carried out to find the optimum operative conditions to maximize the production of acrolein, the main compound of glycerol dehydration. The first of these, is performed starting from a temperature of 300 °C, to make sure that the input steam conditions. In fact, glycerol has a boiling temperature of 290 °C.

Following the reaction section, the purification phases take place: multistage compression, flash, adsorption and distillation. The flash temperature (FLASH-1 in Fig. 6) is 48 °C compatible with the use of cooling water and the pressure is 10 atm, allowing an 85% recovery of

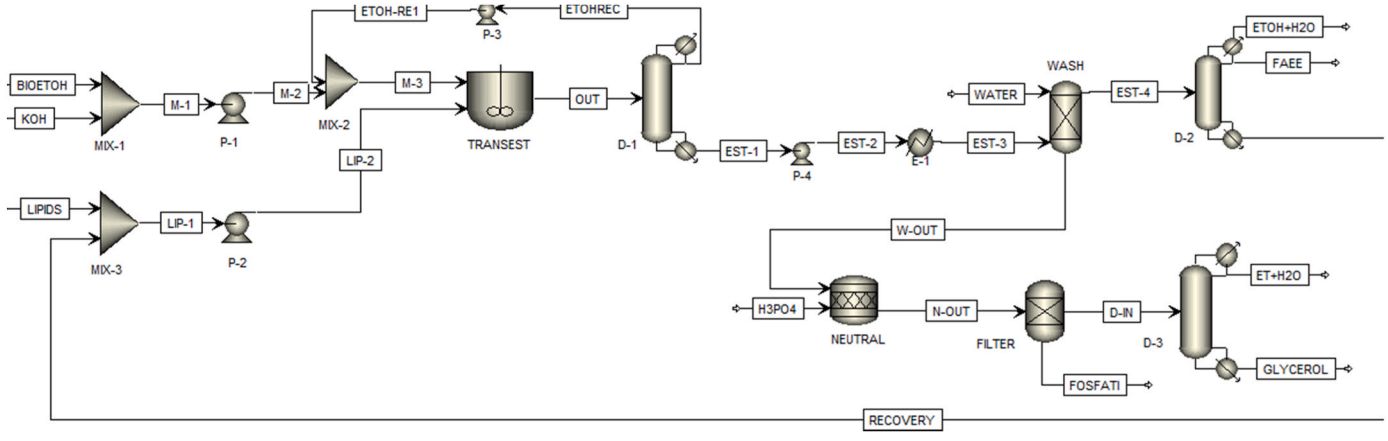

Fig. 5. Biodiesel production unit modelled in the simulation software.

Table 3
Catalyst data zeolite HZSM-5.

	Value	Units
Catalyst Density	720	kg/m^3
Si/Al ratio	38	–
Void fraction	0.75	–
Catalyst to oil ratio	5.4	kg/kg
Catalyst deactivation energy	67 210	kJ/kmol
Catalyst specific heat	1	kJ/kgK

acetaldehyde in the liquid stream. The gas phase from the flash is further cooled to 35 °C and sent to an absorption column with a water stream to maximize the separation of non-condensable compounds. The column (ABSORP in Fig. 6) was modelled using the RadFrac simulation block, with 10 stages and a head temperature of 25 °C. Separation units operating parameters are from (Banu et al., 2015).

Hydrogen is separated from the non-condensable through PSA, representing a product. On the other hand, the liquid streams from the first flash and the bottom of the absorption column, are mixed and sent to the distillation unit. The previous steps make it possible to obtain a distillation feed with at least 95% of the compound of interest (acrolein and acetaldehyde). The last separation step is dehydration, carried out using a distillation column (D-1 in Fig. 6) with 10 stages, reflux ratio 0.48 and operating at atmospheric pressure. A recovery of 99.9% of the compounds of interest in the head was obtained, through the acrolein-water azeotrope, which has a molar composition of 91.1% acrolein and 8.9% water. The residue recovered from the bottom is recirculated, after pumping (P-2 in Fig. 6) and cooling (E−6 in Fig. 6), to the top of the absorption column.

Fig. 6 displays the acrolein purification train.

The ammonia stream from its production section expands to atmospheric pressure before being mixed with the distillate stream and the recirculating stream. The inlet conditions for the pyridine synthesis reactor are 250 °C and 1 atm. The reactor operates with an ammonia molar flowrate 12 folds larger than that of glycerol entering in the dehydration section and at a temperature of 550 °C (L. Xu et al., 2015), which must be lowered before entering the compressor for the purification stage. So, to achieve these two targets, a train of heat exchangers (E−7, E−8, E−9 in Fig. 7) is realized to maximize heat recovery.

The reactions considered are (equation (10) and (11)):

$$C_3H_4O + C_2H_4O + NH_3 \rightarrow C_5H_5N + 2\,H_2O + H_2 \quad (10)$$

$$2\,C_3H_4O + NH_3 \rightarrow C_6H_7N + 2H_2O \quad (11)$$

Fig. 7 shows the Pyridine synthesis section.

A purification train follows the pyridine production one. The flash unit (FLASH-2 in Fig. 7) operating conditions are 20 atm and 45 °C, achieved by an inter-refrigerated multi-stage compressor. These conditions make it possible to recover most of the non-condensable gases (98%) and ammonia (80%) in the gas stream, while pyridine with 3-picoline, the main by-product, are present in the liquid stream with the residual ammonia. The gaseous mixture containing carbon monoxide, ammonia and hydrogen undergoes to two sequential PSA operations at 15 atm of pressure (Rispoli et al., 2021a). The first one (PSA-2 in Fig. 7) allows to obtain hydrogen at 99% of purity, also considered as a product, while the second (PSA-3 in Fig. 7) allows the separation of carbon monoxide, always with 99% of purity, so that only ammonia is recirculated.

To maximize the ammonia recovery and to reduce the make-up, a distillation operation (D-2 in Fig. 7) at 15 atm is carried out with 7 stages and a reflux ratio of 0.2, allowing the separation of the residual ammonia from the pyridine mixture. The useful ammonia flowrate at the inlet of the section is 124 kmol/h.

Finally, an additional distillation column (D-3 in Fig. 7) operating at atmospheric pressure with 15 stages and reflux ratio of 2.23, is adopted to separate the target product, obtaining a pyridine flowrate of 107.4 kmol/h.

Fig. 7A in supplementary material shows the Pyridine purification section.

3. Processes analysis

As previously mentioned, every analysis in this work was studied for two scenarios:

- Scenario 1: the stream (POST-EXT in Fig. 5A) obtained after the extraction is not valorised in the cycle, since the bioethanol is not produced in excess with respect to the target biodiesel productivity of 300 t/h.
- Scenario 2: the stream (OFMSW-2 in Fig. 5A) obtained after the extraction is upgraded into a fermentation unit to produce additional bioethanol, which is an additional product of the plant.

3.1. Energy analysis

This analysis is based on the first principle of the thermodynamic and allows to evaluate the energy yield of the entire process.

The global energy efficiency is defined as ratio between energy leaving the system and the one entering in it, as reported in equation

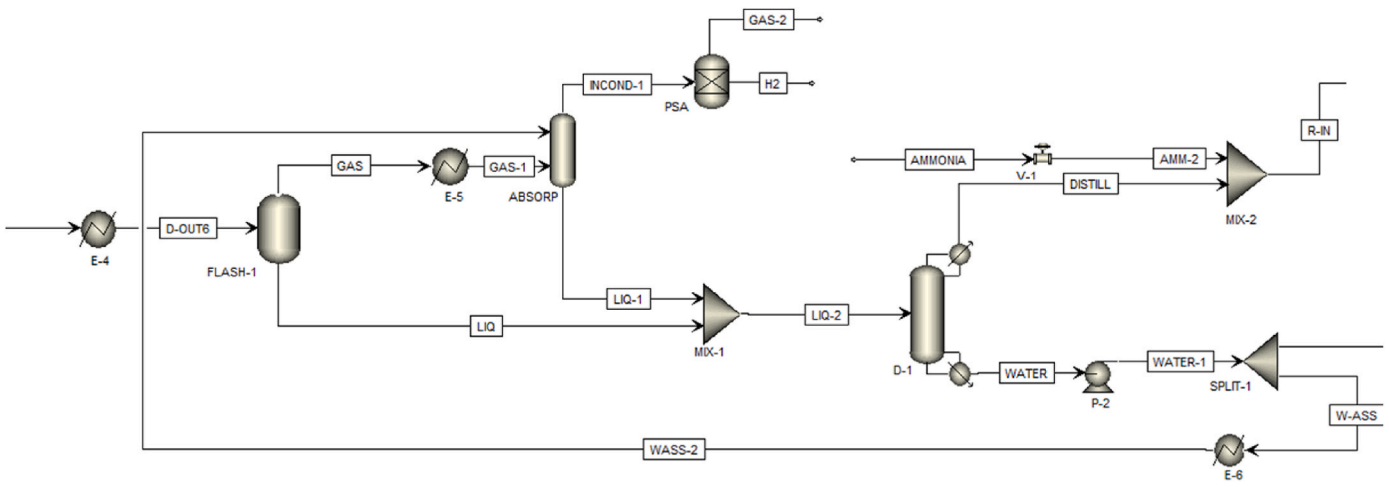

Fig. 6. Acrolein purification section modelled in the simulation software.

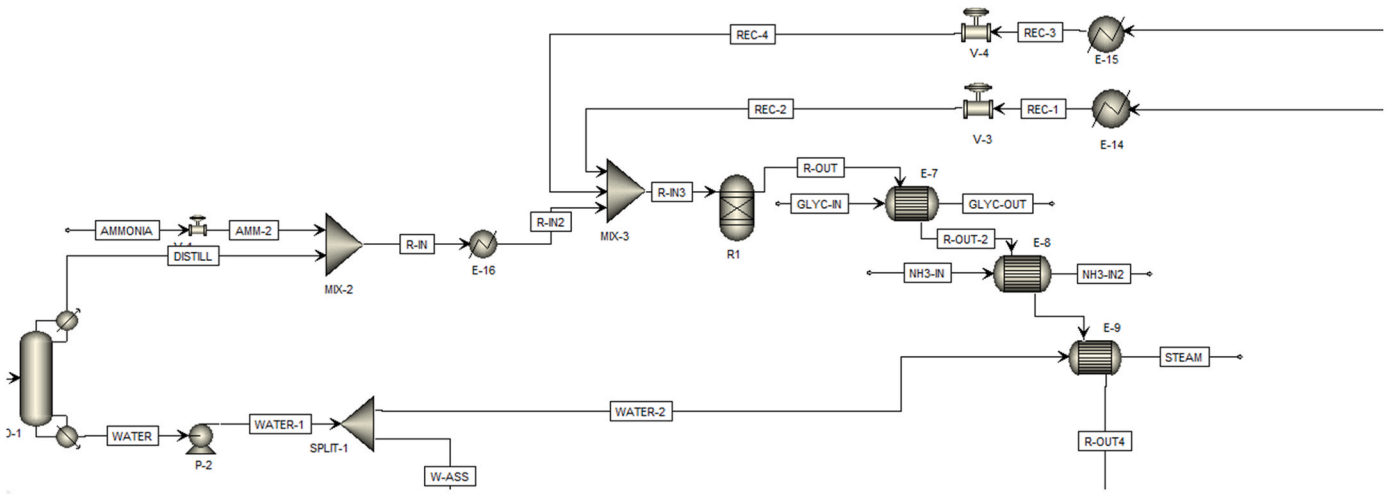

Fig. 7. Pyridine synthesis section modelled in the simulation software.

(12) (Nižetić et al., 2018):

$$\eta_{en} = \frac{output\ energy}{input\ energy} = 1 - \frac{energy\ loss}{input\ energy} \tag{12}$$

The efficiency can be also evaluated as follows (eq. (13)) (Nižetić et al., 2018):

$$\eta_{en} = \frac{\sum F_{product} \cdot LHV_{product}}{P + \sum F_{feed} \cdot LHV_{feed}} \tag{13}$$

where $F_{product}$ [kg/s] is the flowrate of all the streams going out from the system, F_{feed} [kg/s] is the flowrate of all the streams entering into the system, $LHV_{product}$ and LHV_{feed} are their lower heating value [MJ/kg], and P [MW] is the total power absorbed required by all the operating machines (like pumps and compressors).

3.2. Exergy analysis

The exergy analysis is based on the second principle of the thermodynamic. For the calculation, the authors used as reference state 25 °C and atmospheric pressure (Kotas, 1985).

The total exergy of the streams can be evaluated as a sum of three contributes (Kotas, 1985):

- Physical exergy, which is the maximum work can be obtained from the delta temperature and pressure between the entering stream and the environment. It is calculated in the aspen plus simulation environment with equation (14):

$$Ex^{ph}_{in-out} = M_{in-out} \cdot [(H_i - H_0) - T_0 \cdot (S_i - S_0)] \tag{14}$$

The subscripts in and out indicate feed or product stream.

- Mechanical exergy, which is the maximum work available from kinetic energy and potential energy. It was neglected, since it is irrelevant with respect of the other two components.
- Chemical Exergy, which is the maximum work available from the delta composition between stream and environment and it is evaluated as follow (eq. (15)):

$$Ex^{ch}_{in-out} = M_{in-out} \cdot \left[\sum_n x_i \cdot ex^0_i + R \cdot T_0 \cdot \sum_n x_i \cdot \ln(x_i) \right] \tag{15}$$

The subscripts in and out indicate feed or product stream. Regarding the values of the standard exergy of the species, the authors used the ones reported in literature (Morris and Szargut, 1986).

Regarding the fluid machinery present in the system, their exergy is equal to their absorbed power [kW] (Kotas, 1985).

At this point, an exergetic efficiency can be defined as reported in equation (16):

$$\eta_{ex} = \frac{Ex^{tot}_{prod}}{Ex^{tot}_{feed} + Ex_{machines}} \tag{16}$$

For this analysis it is important to evaluate the destructed exergy and the waste exergy, defined in the equation (17):

$$Ex^{tot}_{d} = Ex^{tot}_{feed} - Ex^{tot}_{prod} = Ex^{tot}_{waste} + irreversibility \tag{17}$$

whereas irreversibility term [kW] depends on the generated entropy.

Finally, the exergy efficiency can be also expressed as reported in equation (18):

$$\eta_{ex} = 1 - \frac{Ex^{tot}_{d}}{Ex^{tot}_{feed}} \tag{18}$$

The goal of this analysis is to maximize the exergy yield, by reducing the destructed exergy by exergy waste or irreversibility reduction, usually leading to a real minimization or valorization of waste streams (Marandi et al., 2021; Pan et al., 2021).

3.3. Environmental analysis

The environmental analysis has as a goal the evaluation of the carbon footprint of the entire system proposed. It is based on the calculation of the global emission of the carbon dioxide both as it is and as carbon dioxide equivalent, due to emission of other polluting products (Rispoli et al., 2021a) or due to the power consumptions.

The entire analysis is based on the "carbon neutrality" hypothesis, which affirms the CO_2 emitted starting from waste as feed has not to be considered in term of carbon tax contributes (Abdallah et al., 2018).

As far as the CO_2 equivalent for the power production is concerned, the Italian energy mix correlation factor, equal to 0.29 $kgCO_2$/kWh was adopted. Both the CO_2 emitted in the atmosphere with the lipids' stream and the one produced from the combustion of the natural gas in the gasification reactor have been considered (Rispoli et al., 2021a).

3.4. Economic analysis: opex

In the economic analysis the Operative Cost (OpEx) of the plant have been evaluated.

These costs are divided in four main categories:

- Purchase cost of the raw materials: in this item are present the reactants necessary for the process, like phosphoric acid, methane and potassium hydroxide. The values, reported in Table 5A in supplementary material, were found in literature (Turton et al., 2012).
- Utilities cost: this item includes the contributes of the power and cooling and heating mediums. In Table 6A in supplementary material, the unitary cost for each utility is reported (Turton et al., 2012).
- Waste-water treatment cost: Table 7A in supplementary material reports the cost associated to waste gas, PSA adsorption and digestate disposal (Turton et al., 2012).
- Manpower cost: for the esteem of the manpower cost, first of all the number of operators necessary for each work shift should be evaluated (eq. (19) (Turton et al., 2012)):

$$N_{OL} = \left(6.29 + 31.7 \cdot P^2 + 0.23 N_{np}\right)^{0.5} \quad (19)$$

Then, it was considered that an operator works 8200 h/y, 8 h/d and 5 d/week (Turton et al., 2012) and for this reason 4.5 operators are necessary to cover a work shift 24/7.

The cost of the manpower can be evaluated as reported in equation (20):

$$C_{OL} = salary \cdot 4.5 \cdot N_{OL} \quad (20)$$

An average salary of 75 × 10^3 USD/y (Max S. Peters and Klaus D. Timmerhaus, 2003) was adopted.

- Carbon tax: the carbon tax is the cost related to the emission of carbon dioxide in atmosphere. For this analysis, a value of 0.047 USD/kgCO_2 (Rispoli et al., 2021b) was adopted.

4. Results and discussion

In this paragraph, the results of the model will be analysed and commented. In particular, both the results derived from the simulation and from the energy and environmental analysis.

4.1. Simulation results

4.1.1. Gasification and ammonia section

The main product of the gasification reactor is the syngas, exiting from the top, whereas the by-product of the process is a granular solid, exiting from the bottom of the reactor. Their compositions and physical conditions are reported in Table 4. This Table shown that the solid is composed of a mix of oxides while the gases exit from the top. It is possible to see the low hydrogen content compared to CO: for this reason, a water gas shift step is added. The syngas cleaning steps are described in a previous work (Rispoli et al., 2021a).

As said before, the water gas shift step is necessary to rise the H_2/CO ratio. Table 5 reports the composition of the gas exiting from the WGS unit:

The temperature and the conversion of this step were in line with literature data. In particular, (Borgogna et al., 2019) reported that the output temperature of the adiabatic reactor is close to 470 °C while, the conversion of CO is in the range 30.14–64.66% (Hyun Kim et al., 2017). Considering the flowrate of CO entering the water gas shift section (which is the same as that leaving the top of gasification reactor) and the flowrate that leaving the shift, the conversion is calculated as 48.1%. The by-product hydrogen flowrate recovered from this section was equal to 7.94 t/h.

At this point, the Table 6 below reports the composition of the ammonia reactor output:

Operating the reactor under a non-stoichiometric ratio noticeably reduces H_2 intake and increases the recycle load. For these reasons a H_2/N_2 ratio of 3 was chosen (Cheema and Krewer, 2018) and after the condensation performed at 25 °C, the NH_3 recovered is 2.213 t/h, with a hydrogen conversion of 47% and an ammonia yield of 39%.

Table 4
Composition of syngas and granulate exiting from the reactor.

Reactor's product composition			
	Unit	Syngas	Granule
Temperature	°C	1100	2000
Pressure	atm	1.2	1.2
Mass flow	t/h	141.4	26.65
O_2	w/w	0	0
N_2	w/w	0.012	0
Cl_2	w/w	0	0
H_2O	w/w	0.196	0
H_2	w/w	0.041	0
CH_4	w/w	2.5×10^{-6}	0
CO	w/w	0.525	0
CO_2	w/w	0.215	0
COS	w/w	2.4×10^{-4}	0
HCl	w/w	7.1×10^{-3}	0
H_2S	w/w	3.4×10^{-3}	0
NO_2	w/w	0	0
SiO_2	w/w	0	0.36
CaO	w/w	0	0.36
Al_2O_3	w/w	0	0.13
Fe_2O_3	w/w	0	0.15
HCN	w/w	1.11×10^{-7}	1.6×10^{-8}

Table 5
Composition of gas exiting from shift reaction.

Shift reactor output composition		
	Unit	WGS-OUT
Temperature	°C	473.1
Pressure	atm	1
Mass flow	t/h	152
CO	w/w	0.253
CO_2	w/w	0.57
H_2O	w/w	0.111
H_2	w/w	0.055
N_2	w/w	0.011

Table 6
Ammonia reactor output composition.

Shift reactor output composition		
	Unit	NH_3
Temperature	°C	400
Pressure	atm	200
Mass flow	kg/h	5633
H_2	w/w	0.078
N_2	w/w	0.361
NH_3	w/w	0.561

4.1.2. ASU

The flowrate of feed air is 160.11 t/h and temperature of 25 °C. The Table 7 shown the composition of the stream in output from the cryogenic distillation, after the heat recovery and optimization.

From Table 7 it is possible to notice that the N_2 stream has a 96% of purity while O_2 has a 98% of purity. The value obtained for oxygen is within the range given in literature, while the value of nitrogen is assumed a bit lower due to the presence of argon as main impurity that has not been considered for simplicity of simulation (Kroschwitz JI. and Seidel A., 2007).

4.1.3. OFMSW section

Table 8 shows the composition of the stream in output from the extraction unit.

After the extraction there is a split: the flow rate of municipal solid waste that goes to fermentation step is 155 t/h, whereas the other 2487 t/h constitutes the post-extraction waste stream.

Table 7
ASU output composition.

ASU output composition				
	Unit	WN2-1	N2-2	O2-1
Temperature	°C	49.96	49.96	49.96
Pressure	atm	1.3	1.3	1.3
Mass flow	t/h	4.248	118.8	37.03
O_2	w/w	0.087	0.042	0.982
N_2	w/w	0.913	0.958	0.018

The Table 8A in supplementary material reports the composition of the flow post saccharification and fermentation unit. Comparing the two tables it is possible to see that the conversions mentioned in the previous paragraph (Tables 1A and 2A in the supplementary material) have been respected.

After the purification step, a bioethanol flowrate of 54.19 t/h is obtained in the first scenario while 816.9 t/h is obtained in the second (where also the 2487 t/h of post-extraction OFMSW stream has been valorised).

4.1.4. Biodiesel synthesis

Table 9 reports the composition of the product stream leaving the transesterification reactor. As reported in literature (Silva and de Andrade, 2020) the conversion is very high and according to the adopted residence time (1.5 h) a very high yield can be obtained.

A biodiesel stream with a flow rate of 303.12 t/h is obtained from this section, which represents 98% of the ethyl ester flow out of the reactor. While the glycerol obtained is 32.96 t/h that is the 99.5% of the flow out of the reactor.

4.1.5. Pyridine synthesis

Table 9A reports the composition after dehydration step of glycerol. It is possible to see the complete conversion of the glycerol as reported in literature and, also the decrease of the temperature, due to the endothermic reactions that takes place (Banu et al., 2015).

Sensitivity analyses are carried out to establish the optimal temperature of the feed and the sizing of the reactor. As can be seen from the Fig. 8 if the temperature increases, a decrease of acrolein production and an increase in by-products occur. For this reason, a feed temperature at reactor of 300 °C was selected.

While in the Fig. 8A in the supplementary material, the flow rate of acrolein is reported as a function of reactor size, length [m] and diameter [m]. This analysis shown that a small reactor volume is needed to maximize the acrolein yield. This is explained by the kinetics of the reaction: the kinetic constants of the target reactions are much lower than those of the competitive reaction, this means that a low residence time and a small volume are required to achieve the optimum. Based on the results obtained from the sensitivity analysis, the reactor was sized with a length of 0.6 m and a diameter of 0.1 m. Considering that for a PFR the economic optimum is found in a length/diameter ratio between 6 and 25 and that small dimensions are needed in our case a L/D ratio of 6 has been chose.

Table 8
Extraction unit output composition.

Extraction output composition			
	Unit	POST-EXT	OFMSW-2
Temperature	°C	38.38	38.38
Pressure	atm	1	1
Mass flow	t/h	2487	155
Starch	w/w	0.31	0.31
Proteins	w/w	0.179	0.179
Cellulose	w/w	0.241	0.241
Hemicellulose	w/w	0.175	0.175
Tripalmitin	w/w	0.031	0.031
Triolein	w/w	0.036	0.036
Trimyristin	w/w	0.028	0.028

Table 9
Transesterification output composition.

Transesterification output composition		
	Unit	OUT
Temperature	°C	60
Pressure	atm	1.38
Mass flow	t/h	395
Triolein	w/w	1.4×10^{-4}
Diolein	w/w	1.1×10^{-4}
Monoolein	w/w	4.5×10^{-4}
Tripalmitin	w/w	1.4×10^{-4}
Dipalmitin	w/w	1×10^{-4}
Monopalmitin	w/w	4×10^{-4}
Trimyristin	w/w	1.1×10^{-4}
Dimyristin	w/w	1×10^{-4}
Monomyristin	w/w	6.6×10^{-4}
KOH	w/w	7.2×10^{-4}
Ethanol	w/w	0.126
Water	w/w	6.5×10^{-3}
Glycerol	w/w	0.084
Ethyl oleate	w/w	0.292
Ethyl palmitate	w/w	0.257
Ethyl myristate	w/w	0.231

Table 10 shown the composition at the output of the pyridine synthesis reactor. In this step the reactants, acrolein and acetaldehyde, are completely converted into their respective products.

After the purification step, a flowrate of 8.492 t/h of pyridine is obtained, that is 98% of the flowrate out of the reactor.

4.2. Process analysis

4.2.1. Energy analysis

The result of the analysis for Scenarios 1 and 2 are reported in Table 11.

The specific consumption in the first case are 72.14 MJ/kg biodiesel and 2575 MJ/kg pyridine while in the second 12.85 MJ/kg biodiesel, 458.7 MJ/kg pyridine and 4.8 MJ/kg bioethanol. The energy efficiency value increased from 27.4% (Scenario 1) up to.87.1% (scenario 2) because the additional produced bioethanol is considered a new product of the plant (in scenario 1 the residual waste was not valorised). The increase of energy consumption in Fermentation section was less than 30 MW. Basing only on energy analysis, Scenario 2 represents the optimal case. If the energetic efficiency of the proposed plant is compared with other waste disposal treatment, it can be easily seen the convenience: indeed, the efficiency of waste incineration process was calculated around 19% in the study of M ü nster et al. (Münster and Lund, 2010). In this study it was also predicted increasing until a value around 29% in 2050.

4.2.2. Exergy analysis

The chemical exergy of the feed was evaluated using the equation reported in the work of Eboh et al. (2016), considering all the different species from which it is composed, like cellulose, hemicellulose, protein, starch, etc., obtaining a value of 18.28×10^3 MW.

Subsequently, in order to evaluate the exergy efficiency of the plant, the exergy balance for every unit of the plant for both scenarios has been performed. The results are reported in Table 12.

The exergy efficiency of the whole cycle was estimated equal to 30.2% and 84.9% for Scenario 1 and 2. This result is in line with that of the energy analysis, i.e., the Scenario 2 appears more profitable with respect to Scenario 1 because of the residual waste valorization, notwithstanding the larger energy consumptions (and larger exergy fed to the system, less than 4 MW) due to the additional bioethanol production in Fermentation section.

So as to confirm this thesis, also the irreversibility and the exergy

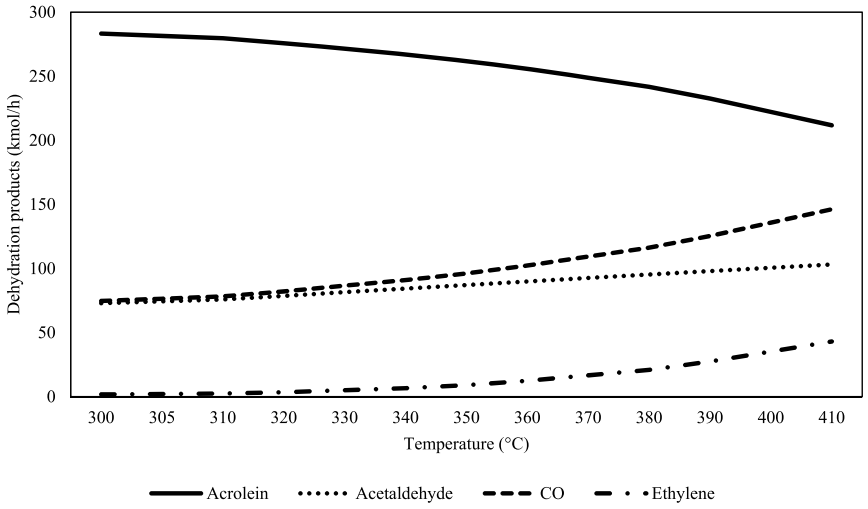

Fig. 8. Temperature sensitivity analysis for acrolein production.

Table 10
Pyridine reactor output composition.

Pyridine reactor output composition		
	Unit	R-OUT
Temperature	°C	550
Pressure	atm	1
Mass flow	t/h	93.68
Glycerol	w/w	0
Ammonia	w/w	0.76
Acetaldehyde	w/w	1.4×10^{-7}
Acrolein	w/w	1.7×10^{-8}
CO	w/w	0.112
Ethylene	w/w	0.005
H_2	w/w	0.013
Water	w/w	1×10^{-4}
Pyridine	w/w	0.1
3-picoline	w/w	0.01

Table 11
Energy analysis.

Energy analysis				
Section	Energy IN scenario 1 (MW)	Energy OUT scenario 1 (MW)	Energy IN scenario 2 (MW)	Energy OUT scenario 2 (MW)
Fermentation	7733	0	7733	4992
Gasification	591	266	591	266
ASU	9	0	9	0
Biodiesel	6	1880	6	1880
Pyridine	23	142	23	142
TOT	8362	2288	8362	7280

Table 12
Exergy balance: comparison of Scenario 1 and Scenario 2.

Exergy analysis		
Values (GW)	Scenario 1	Scenario 2
Exergy IN	20.2	23.9
Exergy OUT	6.1	20.3
Waste	12.7	1.5
Irreversibility	1.4	2.1

waste streams of the plant have been evaluated.

Fig. 9 reports a comparison between the two scenarios, considering Exergy IN, Exergy OUT, Waste and Irreversibility.

The destructed exergy due to waste streams in Scenario 1 is about 1 order of magnitude higher with respect to that of Scenario 2, clearly indicating the larger profitability of the second case. Conversely, the irreversibility term of Scenario 2 was higher (2.13 MW) with respect to the first scenario (1.27 MW), because of the larger energy consumptions (and larger fluid flowrates elaborated by fluid machinery and units) in the Fermentation section. However, this difference is not similar to that related to waste exergy term.

The exergy efficiency of the first scenario is a result of absolute relief if it is compared to the ones found in literature of a similar plant that treats civil waste: for example, the waste to energy plant studied in a previous work (Rispoli et al., 2021c) presented an exergy efficiency of around 22%. Moreover, the authors compared the results with their previous work (Rispoli et al., 2021c) where a thermal conversion process of the waste into energy and the carbon dioxide contained in the waste flue gases was recovered and converted in methane with the addition of an hydrogen stream from water electrolysis; both the precedent work and the first scenario of the present one present an exergy efficiency slightly higher than 30%.

4.2.3. Environmental analysis

In the environmental analysis the global carbon dioxide emissions have been evaluated, taking into account the contribution due to equivalent emissions related to energy consumes and those related to the emission of the fermenter.

As concerned the first scenario, for the carbon dioxide emitted a value of 166.2 t/h was estimated. On the other hand, for the second scenario, the carbon dioxide emitted for the upgrading of the bioethanol stream going out from the fermentation unit is notable higher; for this reason, the analysis returned a value of 986.1 t/h.

The goal of this analysis was to evaluate the carbon footprint of the whole cycle, expressed as kg CO_2/kg product. The results are shown in Fig. 10.

As reported in Fig. 10, the pyridine, that is the main product of the plant, in Scenario 2 has a carbon footprint (116.1 kg CO_2/kg pyridine) of 1 order of magnitude higher with respect to that of Scenario 1 (21 kg CO_2/kg pyridine); analogous considerations can be drawn for the carbon footprint of Biodiesel (3.25 kg CO_2/kg biodiesel in scenario 2 versus 0.55 kg CO_2/kg biodiesel in scenario 1).

From what concerns this analysis, the scenario 1 must be preferred

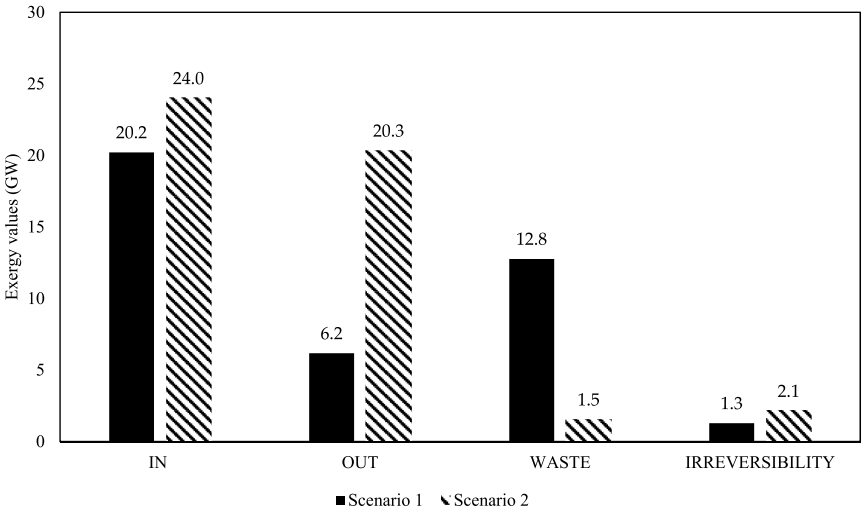

Fig. 9. Exergy balance: subdivision of exergy in IN, OUT, Waste and Irreversibility.

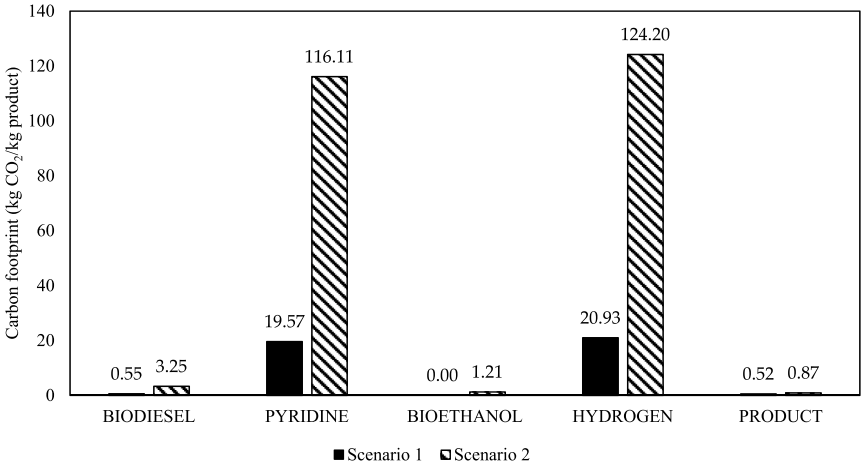

Fig. 10. Carbon footprint results.

with respect to the scenario 2.

Considering a Lower Heating Value for the Biodiesel of 38 MJ/kg (Tesfa et al., 2013), its carbon footprint is equal to 14.5 g CO_2/MJ for the first scenario and 85.5 g CO_2/MJ for the second scenario. Focusing the attention on the first scenario, that will be the preferred one both for what concerns this analysis and for the results of the economic analysis (as reported in the next section), the carbon footprint is notably lower than that obtained according to other production processes: it is 41 g CO_2/MJ by hydrothermal gasification way, 86 g CO_2/MJ through anaerobic digestion and through gasification – power generation it raised up to 109 g CO_2/MJ (Azadi et al., 2014).

4.2.4. Economic analysis

As far as the OpEx analysis is concerned, starting from the unitary values reported in Table 13, the costs related from the utility consumption for every section of the plant has been calculated. In Table 13 the results for both scenarios 1 and 2 are reported.

Table 13 briefly shows that the only difference between the two scenarios, i.e., the valorization of the stream POST-EXT in Fig. 5A, is reflected in this analysis only in the operative cost of the fermentation unit.

Fig. 11 displays the comparison of each operative cost voice for the two analysed scenarios.

Table 13
OpEx results.

Operational cost results			
Section	Scenario 1	Scenario 2	unit
Fermentation	360.3	1308	M USD/y
Gasification	0.5	0.5	M USD/y
ASU	0.03	0.03	M USD/y
Biodiesel	8.1	8.1	M USD/y
Pyridine	27.9	27.9	M USD/y
Energy	55.57	55.57	M USD/y
Operational Total Cost	**452.4**	**1400.2**	**M USD/y**

According to the results reported in Fig. 11, the Scenario 2 resulted less profitable from the OpEx viewpoint, mainly due to the larger utility consumption in the Fermentation section.

On the bases of only the operative cost, the operating production cost of all the products of the proposed work has been estimated and reported in Fig. 12.

These values, without capital expenditure CapEx, are predictive indications only from an operating cost perspective. Therefore Fig. 12 on

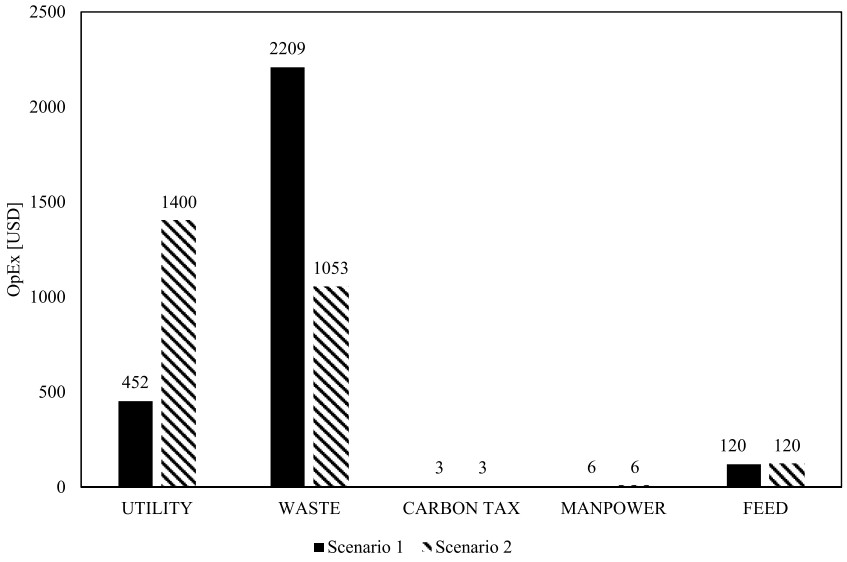

Fig. 11. Operative Cost of the plant Comparison.

production operating costs allows the authors to suggest products that have relatively low operating costs based on the production configurations sought, but requires further attention for profitability estimates. As already mentioned, a more detailed economic analysis, including the calculation of capital costs and profitability will be carried out in the subsequent work.

For every product of the plant, the operating production cost is notably higher in the second scenario with respect to the first one. This means that the first scenario resulted a more attractive cycle from the economic viewpoint, also considering the lower size of the units in the Fermentation section, that certainly will also reduce the capital expenditures (not evaluated in the present work).

Both scenarios return a good value for pyridine operating production cost, although its purchase cost is highly variable depending on its purity, the range is 10–200 USD/kg ("Pyridine Prices," 2020).

Regarding biodiesel operating production cost, the first scenario makes this product very attractive on the market; indeed, Harahap et al. (2019) reported a cost of biodiesel from biorefinery (with palm oil as feed) of around 0.75 USD/kg. Moreover, Sun et al. studied the production of biodiesel trough photoautotrophic algae - based process, evaluating a cost range of 2.7–3.3 USD/kg (Sun et al., 2011): both values reported in literature were considerably higher with respect to the one evaluated in this work. The last item must be considered related to the cost of the products in this work is the hydrogen cost: indeed, today the cost of the "grey hydrogen", that is the hydrogen produced from methane steam reforming, is around 1.5–3 USD/kg (Kaiwen et al., 2018; Yukesh Kannah et al., 2021).

In an energy transition and carbon footprint reduction perspective, the cost of the carbon dioxide emission, also known as carbon tax, will increase in the years, to penalize all the polluting process (as steam reforming) and to encourage all the green process (as the one described in this article). For this reason, the authors are strongly confident that adopting the suggested configurations, green technology is fostered although the overall profitability of doing this would depend on factors

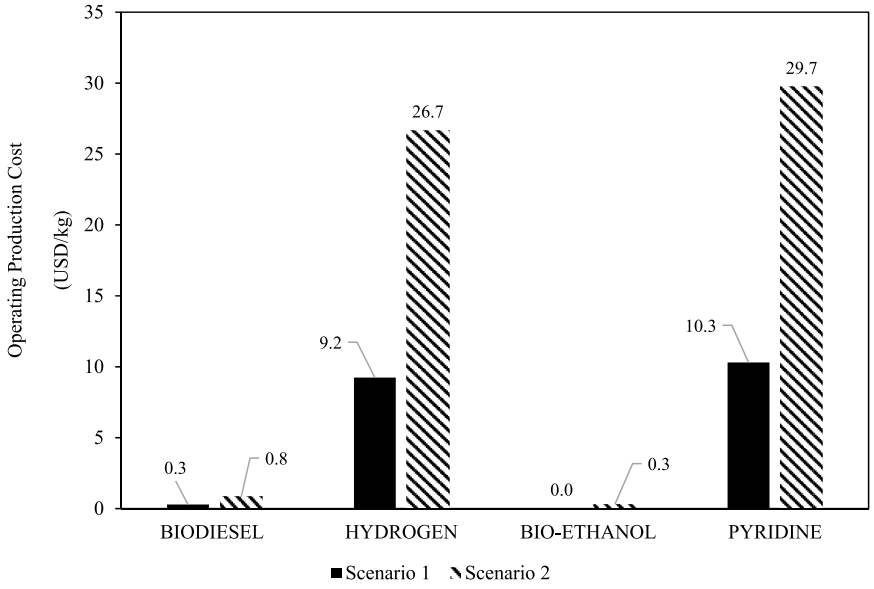

Fig. 12. Operating Production costs of target products.

such as carbon tax.

This is a prediction, because an increase in carbon taxes allows the incentive of low-emission green processes, favouring their diffusion. This policy aims to encourage emission reduction and adoption of environmentally friendly practices. Carbon taxes are designed to internalize the external costs associated with carbon emissions by assigning a monetary value to each ton of CO_2 emitted. By increasing the cost of emitting carbon, carbon taxes provide a financial incentive for businesses and individuals to reduce their carbon footprint. This, in turn, encourages the adoption of cleaner technologies and practices.

Taking this into account, it is estimated that in the not-too-distant future, the implementation of green technologies such as the one proposed in the manuscript could be incentivized by overall lower costs thanks to low CO_2 emissions.

5. Conclusions

In this study an integrated waste management - fine chemicals production plant has been developed and analysed, considering every section required to transform both MSW and its organic fraction into pyridine and biodiesel. Two scenarios were analysed which stand out for the presence of a bioethanol stream, that in the second one was upgraded as by-product. In fact, the simulation has returned a post-extraction waste stream of very high flow rate that could be reused as it still contained biodegradable substrates and, for this reason, the second scenario has been added in order to obtain an additional product, which is bioethanol. Then, the study focused on four fundamental analyses: environmental and exergy analysis showed a higher efficiency for the second scenario, because of the minimization of the waste streams, but the economic and environmental analysis returned better results for the first scenario, since they showed a notable lower carbon footprint and operating cost with respect to the second scenario. The results showed an energy and exergy efficiency of 0.274 and 0.302, for the first scenario whereas 0.871 and 0.849, respectively, for the second one. Moving on, the environmental analysis showed in the first scenario a carbon footprint of 0.52 kg CO_2/kg products, whereas in the second scenario the carbon footprint resulted equal to 0.87 kg CO_2/kg products.

The OpEx analysis showed an increase of the operating cost per unit of product for all the products exiting from the plant moving from the scenario 1 to the scenario 2: indeed, the cost of biodiesel increased from 0.285 USD/kg to 0.822 USD/kg, the cost of hydrogen from 9.24 USD/kg to 26.66 USD/kg and the cost of pyridine from 10.3 USD/kg to 29.73 USD/kg.

In the present work, no estimates were made of the capital costs that could be amortized to arrive at an estimate of the real production costs, which will be realized in a full economic analysis in future work.

In the end it can be stated that waste is a valuable raw material for the development of remarkable processes, representing a good example of circular economy: the life cycle of products is extended, helping to reduce the production of discards. At the same time there is a dual benefit beyond the environmental one, which is the economic one. In fact, as can be seen from the analysis carried out, it is estimated that the operating costs of producing the products will be advantageous compared to those of the market.

The work presented is interesting and innovative thanks to the integration of two processes: gasification for the non-recyclable fraction of the waste, and an extraction and fermentation process for the organic fraction, to obtain the complete conversion of the waste into products with high added value, through an integrated, efficient and low-emissions process.

6. Recent developments and future directions

In this section, it was decided to critically evaluate the global biomass and waste potential, research and development trends, practical implementations, new biomass waste management, pre-treatment and valorization techniques.

The type of process to be implemented depends on many factors, such as: (1) biomass and waste type, (2) conversion technology, (3) targeted end-product, and (4) feasibility (economic, environmental, social, political, etc.).

Comprehensive reviews on production of value-added, platform, specialty and fine chemicals from renewable resources are documented in these papers (Bender et al., 2018; De Corato et al., 2018; de Jong and Gosselink, 2014; Jing et al., 2019; Kohli et al., 2019; Kumar et al., 2018; Liguori et al., 2013; Liu et al., 2019; Matharu et al., 2016; Menon and Rao, 2012; Pachapur et al., 2016; Teigiserova et al., 2019; Xiong et al., 2019; Zhou et al., 2011; Dessie et al., 2020).

One significant hurdle in the development of a bio-based economy is the need for extensive production on a large scale. Regrettably, most of the recent research in this field has been limited to laboratory experimentation. Nevertheless, it's crucial to scale up production significantly in order to establish a competitive bio-based system. Consequently, the prevailing research and development trends should prioritize the progression from laboratory-scale production to pilot projects, demonstrations, and ultimately, large-scale production (Dessie et al., 2020). To help this aspect, process modeling and simulation can make the difference, evaluating different operating conditions, innovative combinations and obtaining interesting performances.

Novel R&D in the field of industrial biotechnology is enabled by diverse scientific and engineering advances. A notable limitation of widely used waste-to-chemical processes is their significant energy consumption, leading to increased production expenses. The central focus of research in this field has been and will continue to be the exploration of more affordable energy sources and energy-efficient methods for converting waste biomass.

Recent review by Saqib et al. proposed hydrothermal carbonization particularly for valorization of food waste as the technique requires relatively low temperature (180–350 °C) and wet feedstock (Saqib et al., 2019). On the contrary, commonly employed techniques such as incineration and pyrolysis need higher temperature (400–550 and 300–1200 °C, respectively) and substrates with low moisture content; which lead to additional processing step and energy cost (Gonçalves et al., 2019; Guerra et al., 2015; Guerra et al., 2018).

Comparatively, production of value-added products through microbial process is regarded as one of the greenest technologies (Bardhan et al., 2015; Tao and Xu, 2009). This is in fact due to cell factories of microorganisms are designed for vigorous conversion selectivity and adaptability, need relatively modest facilities, and can be easily manipulated for specific purpose (Straathof et al., 2019).

It is obviously not easy to shift from the well-established fossil-based economy to the emerging bioeconomy. The underlining challenges include, but not limited to, decentralization of biomass supply chain, technological barrier, dearth of large-scale production, and high initial investment (Dessie et al., 2020).

The primary goal should be to concentrate efforts on creating efficient and ideal methods for treating waste and biomass to address the current challenges. Similarly, in recent years, increasing desires are shown in the development of continuous processes for the commercial-scale production of high-value bio-based products with substantial decreases in cost and facility size.

CRediT authorship contribution statement

Andrea Liberale Rispoli: Writing – original draft, Writing – review & editing, Validation, Software. **Chiara Tizzano:** Software, Visualization, Writing – original draft. **Nicola Verdone:** Resources. **Valentina Segneri:** Visualization, Writing – review & editing, Validation, Software. **Giorgio Vilardi:** Conceptualization, Supervision.

Declaration of competing interest

The authors declare that they have no known competing financial interests or personal relationships that could have appeared to influence the work reported in this paper.

Data availability

Data will be made available on request.

Acknowledgement

This work belongs to a research project funded by Sapienza (RM120172A298917B).

Appendix A. Supplementary data

Supplementary data to this article can be found online at https://doi.org/10.1016/j.jclepro.2023.139051.

Abbreviation

OFMSW = *Organic Fraction of Municipal Solid Waste*
RDF = Refuse Derived Fuel
TG = *triglyceride*
DG = *diglyceride*
MG = *monoglyceride*
ETOH = *ethanol*
FAEE = *fatty acid ethyl ester*

Nomenclature and Symbols
Rc_i = *inter − stage compression ratio* [−]
Zi = number of inter-refrigeration [−]
Z_{i+1} = *number of stages* [−]
Rc = *total compression ratio* [−]
k_0 = *pre − exponential factor* [$l/mol \bullet s$]
E_a = activation energy [kcal/mol]
R = *universal constant of the ideal gas* [$J/mol \bullet K$]
T = temperature [K]
T_0 = *referance state temperature* [K]
C_a, C_b = concentration of the reactants involved [mol/l]
p_i = *partial pressure of each reagent* [atm]
F_{feed} = *flowrate of all streams entering into the system* [kg/s]
$F_{product}$ = *flowrate of all streams going out from system* [kg/s]
LHV_i = *lower heating value of current i* [MJ/kg]
P = *totale power absorbed required by all the operating machines* [MW]
$Ex_{in-out^{ph}}$ = *physical exergy* [kW]
$Ex_{in-out^{ch}}$ = *chemical exergy* [kW]
$Ex_{feed^{tot}}$ = *total exergy of the feeds* [kW]
$Ex_{prod^{tot}}$ = *total exergy of the product streams* [kW]
$Ex_{machines}$ = *exergy related to the fluid machinery and auxiliary units* [kW]
$Ex_{d^{tot}}$ = *destructed exergy* [kW]
$Ex_{waste^{tot}}$ = *waste exergy* [kW]
e^0_{xi} = *standard exergy of the species* [$kJ/kmol$]
M_{in-out} = *molar flowrate entering − exiting from the system* [$kmol/s$]
H_i = *molar enthalpy of the stream i* [$kJ/kmol$]
H_0 = *molar enthalpy at reference state conditions* [$kJ/kmol$]
S_i = *entropy of the stream i* [$J/K \bullet mol$]
S_0 = *entropy at reference state conditions* [$J/K \bullet mol$]
n = *number of chemical species present in the stream*
x_i = *molar fraction of the i − th species*
η_{ex} = *exergy efficiency* [−]
N_{OL} = *work shift* [–]
P = *number of phases in the process where solid is treated* [−]
N_{np} = *number of phases in the process where fluids are maanged.*
[−] = *dimensionless*

References

Abdallah, M., Shanableh, A., Shabib, A., Adghim, M., 2018. Financial feasibility of waste to energy strategies in the United Arab Emirates. Waste Manag. 82, 207–219. https://doi.org/10.1016/j.wasman.2018.10.029.

Agarwal, M., Chauhan, G., Chaurasia, S.P., Singh, K., 2012. Study of catalytic behavior of KOH as homogeneous and heterogeneous catalyst for biodiesel production. J. Taiwan Inst. Chem. Eng. 43, 89–94. https://doi.org/10.1016/j.jtice.2011.06.003.

Aghbashlo, M., Hosseinzadeh-Bandbafha, H., Shahbeik, H., Tabatabaei, M., 2022. The role of sustainability assessment tools in realizing bioenergy and bioproduct systems. Biofuel Res. J. 9, 1697–1706. https://doi.org/10.18331/BRJ2022.9.3.5.

Agovino, M., Ferrara, M., Garofalo, A., 2016. An exploratory analysis on waste management in Italy: a focus on waste disposed in landfill. Land Use Pol. 57, 669–681. https://doi.org/10.1016/j.landusepol.2016.06.027.

Ali Altaf, A., Shahzad, A., Gul, Z., Rasool, N., Badshah, A., Lal, B., Khan, E., Khan, E.A., 2015. Review on the medicinal importance of pyridine derivatives. J. Drug Design Med. Chem. 1, 1–11. https://doi.org/10.11648/j.jddmc.20150101.11.

Ardila, Y.C., Figueroa, J.E.J., Lunelli, B.H., Filho, R.M., Maciel, M.R.W., 2014. Simulation of ethanol production via fermentation of the synthesis gas using aspen plustm. Chem. Eng. Trans. 37, 637–642. https://doi.org/10.3303/CET1437107.

Azadi, P., Brownbridge, G., Mosbach, S., Smallbone, A., Bhave, A., Inderwildi, O., Kraft, M., 2014. The carbon footprint and non-renewable energy demand of algae-derived biodiesel. Appl. Energy 113, 1632–1644. https://doi.org/10.1016/j.apenergy.2013.09.027.

Banu, I., Guta, G., Bildea, S., Bozga, G., 2015. Design and performance evaluation of a plant for glycerol conversion to acrolein. Environ. Eng. Manag. J. 14, 509–517. https://doi.org/10.30638/eemj.2015.054.

Barampouti, E.M., Mai, S., Malamis, D., Moustakas, K., Loizidou, M., 2019. Liquid biofuels from the organic fraction of municipal solid waste: a review. Renew. Sustain. Energy Rev. 110, 298–314. https://doi.org/10.1016/j.rser.2019.04.005.

Bardhan, S.K., Gupta, S., Gorman, M.E., Haider, M.A., 2015. Biorenewable chemicals: feedstocks, technologies and the conflict with food production. Renew. Sustain. Energy Rev. https://doi.org/10.1016/j.rser.2015.06.013.

Beiron, J., Montañés, R.M., Normann, F., Johnsson, F., 2020. Combined heat and power operational modes for increased product flexibility in a waste incineration plant. Energy 202. https://doi.org/10.1016/j.energy.2020.117696.

Bender, T.A., Dabrowski, J.A., Gagné, M.R., 2018. Homogeneous catalysis for the production of low-volume, high-value chemicals from biomass. Nat. Rev. Chem. 2, 35–46. https://doi.org/10.1038/s41570-018-0005-y.

Borgogna, A., Salladini, A., Spadacini, L., Pitrelli, A., Annesini, M.C., Iaquaniello, G., 2019. Methanol production from Refuse Derived Fuel: influence of feedstock composition on process yield through gasification analysis. J. Clean. Prod. 235, 1080–1089. https://doi.org/10.1016/j.jclepro.2019.06.185.

Brunner, P.H., Rechberger, H., 2015. Waste to energy - key element for sustainable waste management. Waste Manag. 37, 3–12. https://doi.org/10.1016/j.wasman.2014.02.003.

Buah, W.K., Cunliffe, A.M., Williams, P.T., 2007. Characterization of products from the pyrolysis of municipal solid waste. Process Saf. Environ. Protect. 85, 450–457. https://doi.org/10.1205/psep07024.

Cheema, I.I., Krewer, U., 2018. Operating envelope of Haber-Bosch process design for power-to-ammonia. RSC Adv. 8, 34926–34936. https://doi.org/10.1039/c8ra06821f.

Cheng, J.J., Timilsina, G.R., 2011. Status and barriers of advanced biofuel technologies: a review. Renew. Energy 36, 3541–3549. https://doi.org/10.1016/j.renene.2011.04.031.

de Jong, E., Gosselink, R.J.A., 2014. Lignocellulose-Based Chemical Products. In: Bioenergy Research: Advances and Applications. Elsevier Inc, pp. 277–313. https://doi.org/10.1016/B978-0-444-59561-4.00017-6.

Eboh, F.C., Ahlström, P., Richards, T., 2016. Estimating the specific chemical exergy of municipal solid waste. Energy Sci. Eng. 4, 217–231. https://doi.org/10.1002/ese3.121.

El-Fadel, M., Findikakis, A.N., Leckie, J.O., 1997. Environmental impacts of solid waste landfilling. J. Environ. Manag. 50, 1–25. https://doi.org/10.1006/jema.1995.0131.

Escalante, J., Chen, W.H., Tabatabaei, M., Hoang, A.T., Kwon, E.E., Andrew Lin, K.Y., Saravanakumar, A., 2022. Pyrolysis of lignocellulosic, algal, plastic, and other biomass wastes for biofuel production and circular bioeconomy: a review of thermogravimetric analysis (TGA) approach. Renew. Sustain. Energy Rev. 169 https://doi.org/10.1016/j.rser.2022.112914.

European Council, 2010. Directive 2010/75/EU of the European Parliament and of the Council of 24 November 2010 on Industrial Emissions (Integrated Pollution Prevention and Control). Off J Eur Union. https://doi.org/10.3000/17252555.L_2010.334.eng.

Ferreira, M.C., Meirelles, A.J.A., Batista, E.A.C., 2013. Study of the fusel oil distillation process. Ind. Eng. Chem. Res. 52, 2336–2351. https://doi.org/10.1021/ie300665z.

Grillo, L.M., 2013. Municipal solid waste (MSW) combustion plants. Waste to Energy Convers. Tech. 72–97. https://doi.org/10.1533/9780857096364.2.72.

Harahap, F., Silveira, S., Khatiwada, D., 2019. Cost competitiveness of palm oil biodiesel production in Indonesia. Energy 170, 62–72. https://doi.org/10.1016/j.energy.2018.12.115.

Hyun Kim, S., Don Yoo, Y., Hoi Gu, J., Hyun Kim, M., 2017. Water gas shift reaction characteristics using syngas from. Waste Gasificat. 6, 35–43.

Islam, K.M.N., 2016. Municipal solid waste to energy generation in Bangladesh: possible scenarios to generate renewable electricity in Dhaka and chittagong city. J. Renew. Energy 2016, 1–16. https://doi.org/10.1155/2016/1712370.

Jing, Y., Guo, Y., Xia, Q., Liu, X., Wang, Y., 2019. Catalytic production of value-added chemicals and liquid fuels from lignocellulosic biomass. Chem. https://doi.org/10.1016/j.chempr.2019.05.022.

Kaiwen, L., Bin, Y., Tao, Z., 2018. Economic analysis of hydrogen production from steam reforming process: a literature review. Energy Sources B Energy Econ. Plann. https://doi.org/10.1080/15567249.2017.1387619.

Khalel, Z.A.M., Rabah, A.A., Barakat, T.A.M., 2013. A new cryogenic air separation process with flash separator. ISRN Thermodynamics 2013, 1–4. https://doi.org/10.1155/2013/253437.

Kohli, K., Prajapati, R., Sharma, B.K., 2019. Bio-based chemicals from renewable biomass for integrated biorefineries. Energies (Basel). https://doi.org/10.3390/en12020233.

Kotas, T.J., 1985. The Exergy Method of Thermal Plant Analysis, first ed. Butterworths. Elsevier. https://doi.org/10.1016/C2013-0-00894-8.

Kroschwitz, J.I., Seidel, A., 2007. Kirk-Othmer Encyclopedia of Chemical Technology. Wiley, London.

Kumar, V., Binod, P., Sindhu, R., Gnansounou, E., Ahluwalia, V., 2018. Bioconversion of pentose sugars to value added chemicals and fuels: recent trends, challenges and possibilities. Bioresour. Technol. https://doi.org/10.1016/j.biortech.2018.08.042.

C.S, Lim, Manan*, Z.A., Sarmidi, M.R., 2003. Simulation modeling of the phase behavior of palm oil–supercritical carbon dioxide. JAOCS, J. Am. Oil Chem. Soc. 80, 1147–1156. https://doi.org/10.1007/s11746-003-0834-6.

Liu, C., Wu, S., Zhang, H., Xiao, R., 2019. Catalytic oxidation of lignin to valuable biomass-based platform chemicals: a review. Fuel Process. Technol. https://doi.org/10.1016/j.fuproc.2019.04.007.

Lüdtke, K.H., 2004. Process Centrifugal Compressors: Basics, Function, Operation, Design, Application., Process Centrifugal Compressors. Springer Berlin Heidelberg. https://doi.org/10.1007/978-3-662-09449-5.

Ma, F., Hanna, M.A., 1997. Biodiesel production: a review. Bioresour. Technol. 70, 1–15. https://doi.org/10.1016/s0960-8524(99)00025-5.

Marandi, S., Sarabchi, N., Yari, M., 2021. Exergy and exergoeconomic comparison between multiple novel combined systems based on proton exchange membrane fuel cells integrated with organic Rankine cycles, and hydrogen boil-off gas subsystem. Energy Convers. Manag. 244, 114532 https://doi.org/10.1016/j.enconman.2021.114532.

Martin, M.A., 2010. First generation biofuels compete. N. Biotech. https://doi.org/10.1016/j.nbt.2010.06.010.

Max S, Peters, Klaus D, Timmerhaus, 2003. Plant Design and Economics for Chemical Engineers, fourth ed. McGraw-Hill.

Menon, V., Rao, M., 2012. Trends in bioconversion of lignocellulose: Biofuels, platform chemicals & biorefinery concept. Prog. Energy Combust. Sci. https://doi.org/10.1016/j.pecs.2012.02.002.

Morris, D.R., Szargut, J., 1986. Standard Chemical Exergy of some elements and compounds on the planet earth. Energy 11, 733–755. https://doi.org/10.1016/0360-5442(86)90013-7.

Münster, M., Lund, H., 2010. Comparing Waste-to-Energy technologies by applying energy system analysis. Waste Manag. 30, 1251–1263. https://doi.org/10.1016/j.wasman.2009.07.001.

Nižetić, S., Barbir, F., Papadopoulos, A., Duić, N., 2018. Exergy, energy and environment. Int. J. Hydrogen Energy. https://doi.org/10.1016/j.ijhydene.2018.01.208.

Olguín, E.J., Sánchez-Galván, G., Arias-Olguín, I.I., Melo, F.J., González-Portela, R.E., Cruz, L., de Philippis, R., Adessi, A., 2022. Microalgae-Based Biorefineries: Challenges and Future Trends to Produce Carbohydrate Enriched Biomass, High-Added Value Products and Bioactive Compounds. Biology, Basel. https://doi.org/10.3390/biology11081146.

Onuki, S., Koziel, J.A., Jenks, W.S., Cai, L., Grewell, D., van Leeuwen, H., 2016. Taking ethanol quality beyond fuel grade: a review. J. Inst. Brew. 122, 588–598. https://doi.org/10.1002/jib.364.

Pan, M., Zhang, K., Li, X., 2021. Optimization of supercritical carbon dioxide based combined cycles for solid oxide fuel cell-gas turbine system: energy, exergy, environmental and economic analyses. Energy Convers. Manag. 248, 114774 https://doi.org/10.1016/j.enconman.2021.114774.

Psomopoulos, C.S., Bourka, A., Themelis, N.J., 2009. Waste-to-energy: a review of the status and benefits in USA. Waste Manag. 29, 1718–1724. https://doi.org/10.1016/j.wasman.2008.11.020.

Pyridine Prices, 2020. URL. https://dir.indiamart.com/impcat/pyridine.html. (Accessed 11 October 2022).

Rispoli, A.L., Iaquaniello, G., Salladini, A., Verdone, N., Pepe, M.R., Borgogna, A., Vilardi, G., 2021a. Simultaneous decarbonisation of steel and Oil&Gas industry by MSW gasification: economic and environmental analysis. Energy Convers. Manag. 245 https://doi.org/10.1016/j.enconman.2021.114577.

Rispoli, A.L., Rispoli, G., Verdone, N., Salladini, A., Agostini, E., Boccacci, M., Parisi, M. P., Mazzarotta, B., Vilardi, G., 2021b. The electrification of conventional industrial processes: the use of mechanical vapor compression in an EtOH–water distillation tower. Energies 14. https://doi.org/10.3390/en14217267.

Rispoli, A.L., Verdone, N., Vilardi, G., 2021c. Green fuel production by coupling plastic waste oxy-combustion and PtG technologies: economic, energy, exergy and CO2-cycle analysis. Fuel Process. Technol. 221 https://doi.org/10.1016/j.fuproc.2021.106922.

Safavi, S.M., Richter, C., Unnthorsson, R., 2021. Dioxin and Furan Emissions from Gasification. Gasif. https://doi.org/10.5772/intechopen.95475.

Silva, G.C.R., de Andrade, M.H.C., 2020. Simulation and optimization of CSTR reactor of a biodiesel plant by various plant sources using Aspen plus. Int. J. Chem. React. Eng. 18 https://doi.org/10.1515/ijcre-2020-0085.

Sun, A., Davis, R., Starbuck, M., Ben-Amotz, A., Pate, R., Pienkos, P.T., 2011. Comparative cost analysis of algal oil production for biofuels. Energy 36, 5169–5179. https://doi.org/10.1016/j.energy.2011.06.020.

Tang, Y., Dong, J., Li, G., Zheng, Y., Chi, Y., Nzihou, A., Weiss-Hortala, E., Ye, C., 2020. Environmental and exergetic life cycle assessment of incineration- and gasification-based waste to energy systems in China. Energy 205. https://doi.org/10.1016/j.energy.2020.118002ï.

Tao, J., Xu, J.H., 2009. Biocatalysis in development of green pharmaceutical processes. Curr. Opin. Chem. Biol. https://doi.org/10.1016/j.cbpa.2009.01.018.

Tesfa, B., Gu, F., Mishra, R., Ball, A.D., 2013. LHV predication models and LHV effect on the performance of CI engine running with biodiesel blends. Energy Convers. Manag. 71, 217–226. https://doi.org/10.1016/j.enconman.2013.04.005.

Thomassen, G., Van Dael, M., Van Passel, S., You, F., 2019. How to assess the potential of emerging green technologies? Towards a prospective environmental and techno-economic assessment framework. Green Chem. https://doi.org/10.1039/c9gc02223f.

Turton, R., Bailie, R.C., Whiting, W.B., Shaeiwitz, J.A., 2012. Analysis, Synthesis and Design of Chemical Processes, third ed.

Wang, S., Yan, W., Zhao, F., 2020. Recovery of solid waste as functional heterogeneous catalysts for organic pollutant removal and biodiesel production. Chem. Eng. J. https://doi.org/10.1016/j.cej.2020.126104.

Wang, X., Zhao, F., Huang, L., 2020. Low temperature dehydration of glycerol to acrolein in vapor phase with hydrogen as dilution: from catalyst screening via TPSR to real-time reaction in a fixed-bed. Catalysts 10. https://doi.org/10.3390/catal10010043.

Xiong, X., Yu, I.K.M., Tsang, D.C.W., Bolan, N.S., Sik Ok, Y., Igalavithana, A.D., Kirkham, M.B., Kim, K.H, Vikrant, K., 2019. Value-added chemicals from food supply chain wastes: State-of-the-art review and future prospects. Chem. Eng. J. 375 https://doi.org/10.1016/j.cej.2019.121983.

Xu, L., Han, Z., Yao, Q., Deng, J., Zhang, Y., Fu, Y., Guo, Q., 2015. Towards the sustainable production of pyridines via thermo-catalytic conversion of glycerol with ammonia over zeolite catalysts. Green Chem. 17, 2426–2435. https://doi.org/10.1039/c4gc02235a.

Xu, X., Kim, J.Y., Cho, H.U., Park, H.R., Park, J.M., 2015. Bioconversion of volatile fatty acids from macroalgae fermentation into microbial lipids by oleaginous yeast. Chem. Eng. J. 264, 735–743. https://doi.org/10.1016/j.cej.2014.12.011.

Yukesh Kannah, R., Kavitha, S., Preethi, Parthiba Karthikeyan, O., Kumar, G., Dai-Viet, N.V., Rajesh Banu, J., 2021. Techno-economic Assessment of Various Hydrogen Production Methods – A Review. Bioresour Technol. https://doi.org/10.1016/j.biortech.2020.124175.

Zhao, X., Korey, M., Li, K., Copenhaver, K., Tekinalp, H., Celik, S., Kalaitzidou, K., Ruan, R., Ragauskas, A.J., Ozcan, S., 2022. Plastic waste upcycling toward a circular economy. Chem. Eng. J. https://doi.org/10.1016/j.cej.2021.131928.